



Rapid decrease in Martian crustal magnetization in the Noachian era: Implications for the dynamo and climate of early Mars

R. J. Lillis,¹ H. V. Frey,² and M. Manga³

Received 14 April 2008; revised 5 June 2008; accepted 12 June 2008; published 26 July 2008.

[1] The magnetic signatures and crater retention ages of the 19 largest (>1000 km diameter) impact basins on Mars are examined to constrain the history of the acquisition of crustal magnetization during the Noachian era. The 5 most clearly impact-demagnetized basins are younger than the 14 basins within which lies substantially re-magnetized crust. Poisson analysis shows that the most likely time of this magnetization cessation was 4.115–4.13 Ga (model age) and that it occurred quickly, taking less than 20 Ma. A global decrease in effective crustal magnetic susceptibility due, e.g., to a decrease in the rate of hydrothermal alteration, is one possible explanation. Alternatively, the cessation of post-impact magnetization reflects the rapid death of the Martian dynamo. **Citation:** Lillis, R. J., H. V. Frey, and M. Manga (2008), Rapid decrease in Martian crustal magnetization in the Noachian era: Implications for the dynamo and climate of early Mars, *Geophys. Res. Lett.*, *35*, L14203, doi:10.1029/2008GL034338.

1. Introduction

[2] Mars does not today possess a core dynamo and associated global magnetic field, though strong crustal magnetization implies that one existed in the past [Acuña *et al.*, 1999]. In general, the history of crustal magnetization within Martian impact basins depends on both the duration of the ancient dynamo and the effective magnetic susceptibility of the crust after the impact. A large impact (e.g., Hellas, Argyre) can alter the magnetization of the entire crust over an area comparable to the final size of the impact basin [e.g., Hood *et al.*, 2003]. Excavation can remove magnetized material and heating causes thermal demagnetization within ~0.5–0.8 basin radii [Mohit and Arkani-Hamed, 2004]. Immediately following the impact, as the crust cools, the rocks can acquire thermoremanent magnetization (TRM) with a magnitude positively dependent on the strength of the local ambient magnetic field and the effective susceptibility of crustal materials. Shock from the impact can add or remove net magnetization, depending on this local field and prior magnetization state of the crust. Unmagnetized materials can be magnetized in an external magnetic field through shock remanent magnetization (SRM) and existing magnetization can be reduced or erased

if the minerals are shocked in an ambient field too weak to induce a sufficient SRM [Cisowski and Fuller, 1978]. In addition to magnetization acquired or erased at or immediately following the time of impact, resulting endogenic volcanism can (if an ambient magnetic field is present) produce TRM. Though associated hydrothermal activity will likely not produce much additional TRM [Ogawa and Manga, 2007], it may produce chemical remanent magnetization (CRM), which can be comparably efficient to TRM for a given quantity of single domain magnetite [Scott and Fuller, 2004].

[3] Magnetization acquired through SRM or TRM, and subsequent modification by TRM and CRM, or its absence due to shock and/or thermal demagnetization, is preserved in the crust and the resulting magnetic fields (or lack thereof) can be detected by orbital measurements. Previous studies used low magnetic field magnitudes over the large basins Isidis, Hellas and Argyre, to argue that the core dynamo had ceased by the time of these impacts [Acuña *et al.*, 1999] and likely before most of the construction of Tharsis [Arkani-Hamed, 2004], ~4 Gyr ago. In contrast, Langlais and Purucker [2007] analyzed magnetometer data over Apollinaris Patera and concluded, from its high-latitude modeled paleopole location, that the dynamo might have been active in the late Noachian: 3.7–3.8 Gyr ago, following any Tharsis-driven true polar wander. Their analysis is however subject to the caveat that the modeled magnetization vectors used in determining such paleopoles suffer from inherent nonuniqueness [Biswas, 2005].

[4] In this paper we adopt a systematic and quantitative approach, using the electron reflection (ER) crustal magnetic field map of Lillis *et al.* [2008b] to examine the magnetic signatures of 19 old (>3.8 Ga), large (>1000 km) Martian impact basins. We use these signatures to their crater retention ages [Frey, 2008] to determine the early history of post-impact crustal magnetization on Mars.

2. Crater Retention Ages and Absolute Model Ages of Large Impact Basins

[5] Quasi-circular depressions (QCDs) were identified in MOLA topography and have been associated with both exposed and buried impact structures by Frey [2006]. More recently, crustal thickness maps derived from gravity and topography [Neumann *et al.*, 2004] have been used to identify circular thin-crust areas (CTAs) as possible additional buried impact structures >300 km in diameter. The combined non-redundant population of QCDs (both visible and buried) and CTAs provides the best estimate available of the N(300) crater retention ages (CRAs) for large Martian basins [Frey, 2008]. N(x) is the cumulative number of superimposed craters of diameter > x km per 10⁶ km². Its

¹Space Sciences Laboratory, University of California, Berkeley, California, USA.

²Planetary Geodynamics Laboratory, NASA Goddard Space Flight Center, Greenbelt, Maryland, USA.

³Department of Earth and Planetary Science, University of California, Berkeley, California, USA.

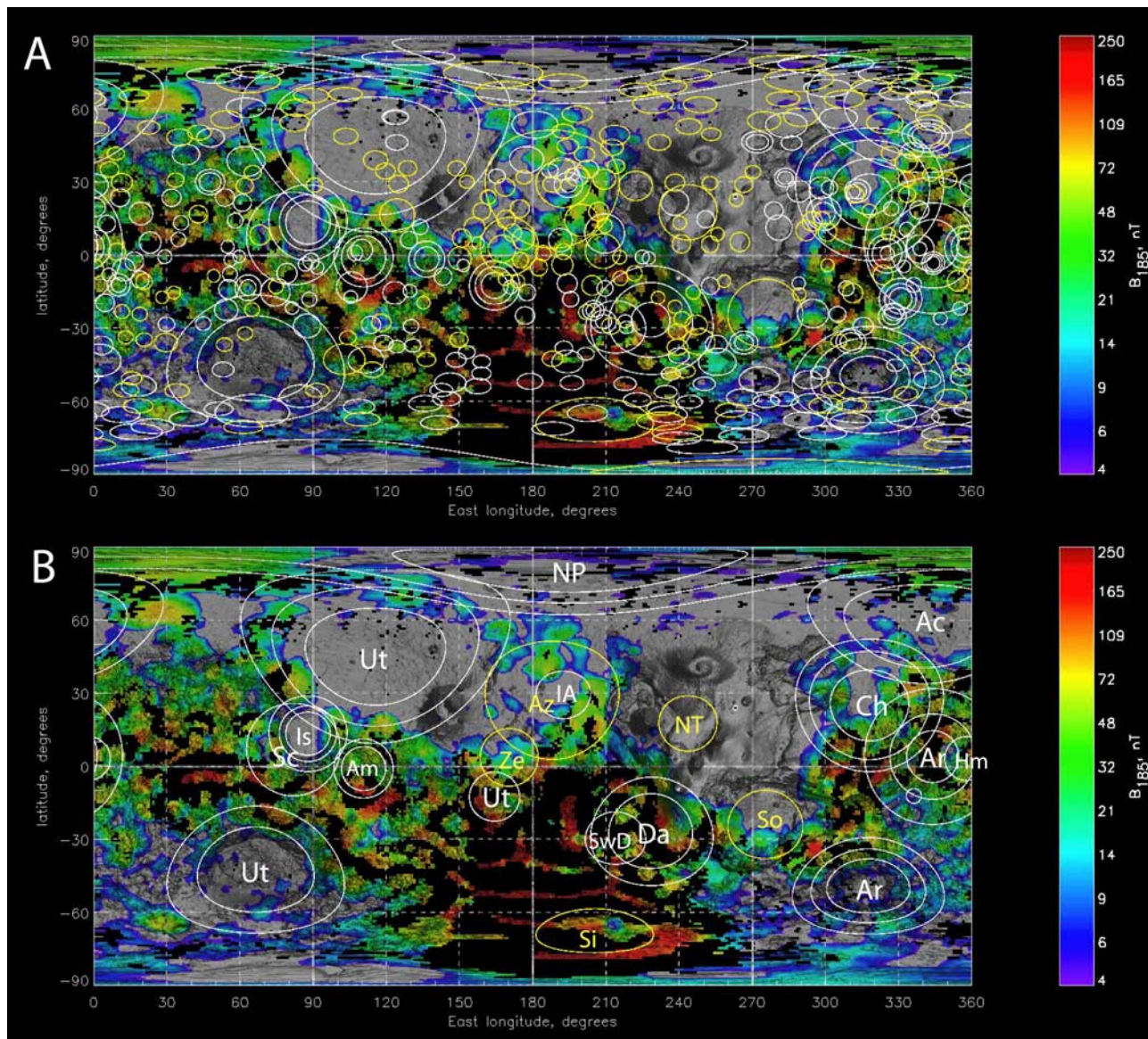


Figure 1. A $0.5^\circ \times 0.5^\circ$ cylindrical projection global map of crustal magnetic field magnitude at 185 km altitude from electron reflectometry, overlaid on shaded MOLA topography. Black pixels represent closed crustal field lines. Details are given by *Lillis et al.* [2008b]. White and yellow circles represent QCDs and non-QCD CTAs respectively [*Frey*, 2008]. (a) All craters >300 km in diameter. (b) Only the 20 large basins used in the study, labeled with abbreviations given in the text.

Poisson uncertainty is given by $(N(x)/\text{basin area})^{1/2}$. CRAs show a strong clustering between $N(300) \geq 2.5$ and 4.0, implying a ‘peak’ in crater production if the CRAs actually reflect formation age. ‘ \geq ’ represents a minimum age because not all subsequently formed craters may be visible.

[6] CRAs can be converted to model “absolute ages” by extrapolating the major stratigraphic boundaries from *Tanaka’s* [1986] small diameter counts using a -2 power law and applying the *Hartmann and Neukum* [2001] (hereinafter referred to as H-N) cratering chronology model ages for these boundaries. If the $N(300)$ relative ages (based on superimposed crater counts) are correct and the conversion to H-N ages is appropriate, then the “absolute” ages of most of the largest basins lie in a very narrow time interval

in Martian history, between 4.1 and 4.2 Ga. See the companion paper by *Frey* [2008] for details.

3. Magnetic Signatures of Large Ancient Impact Basins and Inferred Chronology

[7] Using the technique of electron reflection magnetometry, *Lillis et al.* [2008a; 2008b] produced a map of the magnetic field magnitude $|B|$, due to *crustal* sources only, at 185 km altitude above the Martian datum, hereafter referred to as B_{185} . It has an approximate spatial resolution of ~ 200 km and a detection threshold for crustal fields of $\sim 2\text{--}4$ nT, allowing us to examine the magnetic signatures of impact craters in greater detail than was previously possible. Figure 1a shows the map with circles identifying

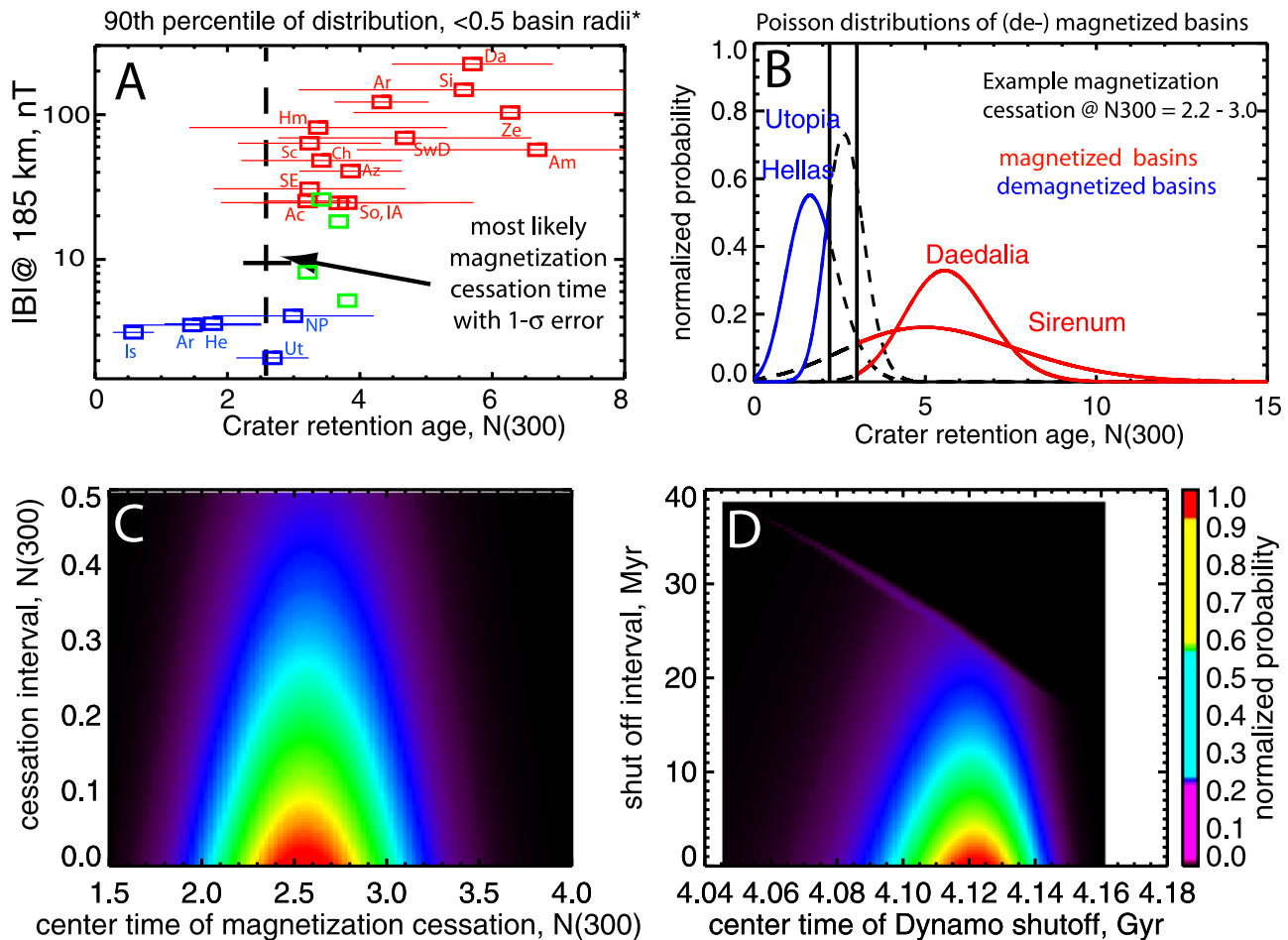


Figure 2. (a) The 90th percentile value of B_{185} inside 0.5 basin radii for the 15 of the 19 largest identified basins is plotted vs. crater retention age $N(300)$. The *0.8 basin radii is the criterion used for the other 4 basins to mitigate the effects of substantial subsequent volcanic (Solis) or impact (Acidalia, Chryse, Inner Amazonis) demagnetization. Green squares show where the four latter aforementioned basins would otherwise have plotted using 0.5 radii. Blue and red represent basins judged to be demagnetized and magnetized respectively. Basins are labeled using abbreviations given in the text. The horizontal error bars represent Poisson uncertainties in CRAs. The 1- σ uncertainty (shown by a horizontal bar) in the likely magnetization cessation time is calculated from the distribution in Figure 2c. The North Tharsis basin is omitted (see text). (b) Poisson distributions of the CRAs of four sample basins. The probability of the cessation happening over an example interval whose minimum duration spanned $N(300) = 2.2 - 3.0$ (two black vertical lines) is calculated by multiplying together the areas under the demagnetized basins' curves to the left of this range (blue), and the areas under the magnetized basins' curves to the right (red), i.e., the probability that all the demagnetized basins were formed after this interval and all the magnetized basins were formed prior to it. The black vertical lines are moved left and right appropriately to produce the relative probability results in Figures 2c and 2d. (c and d) Probabilities as a function of the time at which, and the duration over which, the dynamo ceased operating, in terms of CRA and Hartmann and Neukum [2001] model age, respectively.

all QCDs (white) and non-QCD CTAs (yellow) with diameters >300 km [Frey, 2008].

[8] Because of the non-unique relationship between B_{185} measured over a basin and the magnetization contained therein, we conducted simulations of the magnetic field profile expected over a completely demagnetized crater for a range of crater sizes and pre-impact crustal magnetization coherence scales and concluded that B_{185} is an adequate proxy for basin magnetization for the large basins (>1000 km in diameter) in the study. Details are contained in the auxiliary material.¹

¹Auxiliary materials are available in the HTML. doi:10.1029/2008GL034338.

[9] We now consider, in order of decreasing CRAs, the magnetic signatures of 19 impact structures >1000 km in diameter identified by Frey [2008] and shown in Figure 1, providing in parentheses their abbreviations used in Figures 1 and 2. The Amenthes (Am), Zephyria (Ze), Daedalia (Da), Sirenum (Si), Southwest Daedalia (SwD) and Ares (Ar) basins have the highest CRAs and all have strong magnetic signatures, indicating substantial crustal magnetization. Next we consider Amazonis (Az) and Inner Amazonis (IA). The crust here is ~ 30 km thinner than for the six above-mentioned basins [Neumann et al., 2004], so it is not surprising that the magnetic signature is weaker. Despite several large overprinted demagnetized impact craters (300–600 km) within the basins, both still contain substantial

magnetized regions, indicating that post-impact remagnetization occurred.

[10] The bulk of Tharsis has been thermally demagnetized, most likely by long-lived magmatism and underplating [Johnson and Phillips, 2005]. The same is true for any magnetic signature that might have existed for the North Tharsis (NT) basin [Frey, 2008], hence this basin is not useful for constraining the history of post-impact magnetization. The northern half of the Solis (So) basin has been similarly demagnetized, but the southern half remains unaffected and its magnetic signature implies post-impact magnetization.

[11] Hematite (He), Chryse (Ch), and Scopolus (Sc) basins: subsequent impacts have demagnetized substantial regions of the latter two, but the overall character of these three basins is also consistent with post-impact magnetization.

[12] Acidalia (Ac) is somewhat ambiguous. B_{185} is quite low in the basin center and there are substantial fields of up to 70 nT between the inner and outer rings, as one would expect for a large demagnetizing impact. On the other hand, sources as strong as 30 nT exist inside the basin and a substantial fraction of the regions <4 nT could possibly be explained by the ~ 700 km later-formed impact basin slightly northeast of its center. If Acidalia formed in the era of post-impact magnetization, it was likely the last of the giant basins to do so.

[13] The five youngest basins (North Polar (NP), Utopia (Ut), Hellas (He), Argyre (Ag) and Isidis (Is)) all have crustal fields in their centers mostly below the limit of detection for the ER method. The crust in these five basins is considerably thinner than their surroundings and presumably somewhat less likely to hold a significant volume of magnetized material. However the demagnetization appears so complete in these basins, particularly in Utopia, that we conclude that global conditions were no longer conducive to forming any significant post impact magnetization.

4. Giant Basin Magnetic Timeline

[14] While inspection of ER maps of the individual basins is the best way to estimate the magnetization present after the impact but before any subsequent magnetic alteration, it is instructive to plot a ‘magnetic timeline’ of basin magnetic intensity versus $N(300)$. We represent magnetic intensity by the 90th percentile values of B_{185} inside 0.5 basin radii because this provides an estimate of the post-impact magnetization that is relatively immune from subsequent localized impact or volcanic demagnetization, whilst excluding high outliers. This timeline is shown in Figure 2a with North Tharsis omitted. Despite significant uncertainties in the CRAs (shown by the formal counting error bars), there is a consistent separation in age between the mostly magnetized and mostly demagnetized basins.

[15] If CRAs are indeed indicative of formation ages, these data suggest three epochs of detectable basin formation. The six oldest basins formed in the southern hemisphere in the presence of a substantial global magnetic field and high crustal magnetic susceptibility. The next youngest eight basins, with CRAs between $N(300) \sim 3.0$ – 4.0 , also likely formed in the presence of an active dynamo, with lower magnetization possibly reflecting a thinner crust in some of those regions and/or lower susceptibility. Next

appears a sharp decrease in inferred magnetization for the five youngest basins. Interestingly, the Utopia basin has an age very similar to the cluster of eight substantially magnetized basins, yet has a dramatically different magnetic signature, suggesting a rapid change in the ambient magnetic conditions (global field strength or magnetic susceptibility) around $N(300) \sim 2.5$ – 3.0 .

[16] Figures 2b, 2c, and 2d illustrate the relative probabilities of various times at which, and durations over which, crustal magnetization progressed from being substantial to weak or nonexistent. This was done by calculating the Poisson distributions of crater retention ages (from the number of superimposed craters) for the 14 magnetized and 5 demagnetized basins and assuming all the magnetized basins must be older than all the demagnetized basins. This is equivalent to saying the crustal magnetization cessation occurred only once and took some finite time to happen. The most likely CRA for magnetization cessation is $N(300) = 2.57 \pm 0.22$ (i.e., width of 1 - σ red area in Figure 2d) or in terms of an H-N model absolute age, 4.115 to 4.13 Ga. The large number of basins allows us to place a tighter constraint on this age than for any individual basin. Integrating the probabilities of the cessation intervals in Figure 2d for the most likely cessation age results in probabilities of (96%, 67%, 41%, 20%) that the cessation lasted less than (20, 10, 5, 2) Myr respectively.

5. Implications for the Climate and Dynamo of Early Mars

[17] Hydrothermal alteration may have played a significant role in forming Mars’ strongest crustal magnetic fields [Harrison and Grimm, 2002; Scott and Fuller, 2004] and global changes in geochemical environments may affect the acquisition of CRM and be reflected in the magnetization of the impact basins. From permeability-depth studies on terrestrial basalts [e.g., Saar and Manga, 2004] and the lunar crust scaled to Mars [e.g., Clifford and Parker, 2001], such alteration on Mars could create CRM to depths of up to ~ 10 km in post-impact basin crust. Consider the cases of the magnetic minerals hematite, magnetite and pyrrhotite respectively. For impact basins of the size we consider here, the entire depth of crust inside ~ 0.5 , ~ 0.6 , and ~ 0.7 basin radii is heated above the Curie temperature [Mohit and Arkani-Hamed, 2004] and could produce TRM down to the minimum historical Curie isotherm, estimated at depths of ~ 62 km, ~ 55 km and ~ 35 km [Dunlop and Arkani-Hamed, 2005]. Hence, CRM could influence $\sim 16\%$, $\sim 18\%$ and $\sim 29\%$, while TRM could influence $\sim 25\%$, $\sim 36\%$ and $\sim 49\%$ of the magnetizable volume of post-impact basin crust, giving TRM/CRM volume estimate ratios of ~ 1.5 – 2.0 , depending on magnetic mineral. Given the uncertainties involved, we will assume the volumes influenced by TRM and CRM to be roughly equal and consider two possible, somewhat overlapping, scenarios and compare them with Figure 2a.

[18] In the first scenario, a change in the geochemical environment occurred before the dynamo ceased and resulted in a partial or total cessation of CRM. In this case, we should observe a factor of (at most) $1 + f$ decrease in average basin magnetization, where f is the ratio of the efficiency of CRM to TRM for a given quantity of the

dominant magnetic mineral, followed by a decrease to ‘zero’ (i.e., the detection threshold of ~ 3 nT) after the dynamo cessation (which need not occur in our timeline). For this scenario to explain the gradual magnetization decrease around $N(300) \geq 4.0$, f needs to be $>\sim 1-2$, while for it to explain the rapid magnetization cessation at $N(300) \geq 2.6$, f needs to be $>\sim 7-10$. There is considerable uncertainty in this ratio f as it depends on magnetic mineral, domain state and grain size, and need not be uniform in space and time. For a given quantity of single domain magnetite, CRM can in some cases be comparably as efficient as TRM, i.e., $f \sim 1$ [e.g., McClelland, 1996; Scott and Fuller, 2004]. Hence, this scenario could perhaps explain the early gradual magnetization decrease and, given the compounding uncertainties in the value of f , cannot be completely ruled out as an explanation for the sudden cessation.

[19] Analysis of data from the OMEGA instrument on Mars Express suggests a major change in the geochemical alteration environment, from aqueous alteration forming phyllosilicates (‘Phyllosian’ era) to hydrated sulfates and ferric oxides formed in a more acidic environment (‘Theiikian’ era) [Bibring *et al.*, 2007]. This change occurred sometime before the Isidis impact [Mustard *et al.*, 2007] at ~ 3.94 Ga. This transition is consistent with extensive volcanic outgassing of SO_2 and other volatile species that accompanied the formation of Tharsis in the late Noachian [Phillips *et al.*, 2001]. Following the discussion in the previous paragraph, this transition could perhaps be responsible for the gradual decrease or, less likely in our view, the rapid decrease in magnetization.

[20] In the second scenario, at $N(300) \geq \sim 2.6$ (equivalent to an H-N absolute model age of ≥ 4.115 to 4.13 Ga), dynamo action in the core ceased rapidly (<20 Ma) and the global field disappeared. With the global field gone, only very weak pre-existing crustal fields and solar wind-induced fields were available to remagnetize post-impact crust in the 5 youngest large basins, leaving the very weak signatures we observe.

[21] Due to the high and difficult-to-explain CRM/TRM efficiency ratio required to explain the sudden magnetization cessation at $N(300) \geq \sim 2.6$ as a change in magnetic alteration state, our preference is for the death of the dynamo to explain this cessation. This scenario is also consistent with dynamo simulations by Kuang *et al.* [2008], which indicate that, in the subcritical regime, a $\sim 1\%$ reduction in the core magnetic Reynolds number (R_m) can reduce the surface magnetic field strength by ~ 3 orders of magnitude, effectively ending dynamo action, and that R_m must increase by a geophysically implausible $\sim 20\%$ to restart the dynamo. In other words, like the dynamo in our second scenario, the simulated dynamo also shuts off quickly and does not restart. We note that the cessation interval upper bound is $\sim 100-1000$ times greater than the time for the global field to dissipate following cessation of dynamo action: assuming a core radius of 1700 km and using arguments by Stevenson [2003], this duration is ~ 20 ka, well below the ‘‘resolution’’ of crater retention ages.

[22] The Phyllosian-Theiikian (PT) transition may have occurred as early as ~ 4.16 Ga (HN model age for the beginning of the weakening of the magnetization at $N(300) \geq 4.0$) or perhaps earlier or, as mentioned above, as late as

~ 3.94 Ga. If, as we suggest, the abrupt decrease in magnetization reflects the death of the Martian dynamo, the environmental changes inferred from the PT transition would occur between ~ 30 Ma before and $>\sim 180$ Ma after the global magnetic field disappeared, hence likely afterwards. Bibring *et al.* [2006] offer two possible scenarios for changes in surface environments. In one, phyllosilicate weathering occurs in the subsurface. In the other, phyllosilicates formed close to the surface, and the transition to a more acidic environment is also coupled with a decrease in atmospheric pressure. If the dynamo-death interpretation of our magnetization history is true, it is reasonable to speculate that the decrease in pressure (as well as the final, dry ‘‘Siderikian’’ period) results from some combination of atmospheric erosion by giant impacts and the more active early solar wind stripping away an atmosphere with no global magnetic field to protect it [e.g., Jakosky *et al.*, 1994].

[23] **Acknowledgments.** We thank useful reviews from J. Arkani-Hamed, N. Barlow, and an anonymous reviewer, as well as useful communications with Jack Mustard. Supported by NASA MDAP NNX07AN94G.

References

- Acuña, M. H., *et al.* (1999), Global distribution of crustal magnetization discovered by the Mars Global Surveyor MAG/ER experiment, *Science*, *284*, 790–793.
- Arkani-Hamed, J. (2004), Timing of the Martian core dynamo, *J. Geophys. Res.*, *109*, E03006, doi:10.1029/2003JE002195.
- Bibring, J. P., *et al.* (2006), Global mineralogical and aqueous Mars history derived from OMEGA/Mars Express data, *Science*, *312*, 400–404.
- Bibring, J. P., *et al.* (2007), Coupled ferric oxides and sulfates on the Martian surface, *Science*, *317*, 1206–1210.
- Biswas, R. (2005), Nonuniqueness of the modeled magnetization factors used in determining paleopoles on Mars, Ph.D. thesis, South. Ill. Univ. at Carbondale, Carbondale.
- Cisowski, S. M., and M. Fuller (1978), The effect of shock on the magnetism of terrestrial rocks, *J. Geophys. Res.*, *83*, 3441–3458.
- Clifford, S. M., and T. J. Parker (2001), The evolution of the Martian hydrosphere: Implications for the fate of a primordial ocean and the current state of the northern plains, *Icarus*, *154*, 40–79.
- Dunlop, D. J., and J. Arkani-Hamed (2005), Magnetic minerals in the Martian crust, *J. Geophys. Res.*, *110*, E12S04, doi:10.1029/2005JE002404.
- Frey, H. V. (2006), Impact constraints on, and a chronology for, major events in early Mars history, *J. Geophys. Res.*, *111*, E08S91, doi:10.1029/2005JE002449.
- Frey, H. V. (2008), Ages of very large impact basins on Mars: Implications for the late heavy bombardment in the inner solar system, *Geophys. Res. Lett.*, *35*, L13203, doi:10.1029/2008GL033515.
- Harrison, K. P., and R. E. Grimm (2002), Controls on Martian hydrothermal systems: Application to valley network and magnetic anomaly formation, *J. Geophys. Res.*, *107*(E5), 5025, doi:10.1029/2001JE001616.
- Hartmann, W. K., and G. Neukum (2001), Cratering chronology and the evolution of Mars, *Space Sci. Rev.*, *96*, 165–194.
- Hood, L. L., N. C. Richmond, E. Pierazzo, and P. Rochette (2003), Distribution of crustal magnetic fields on Mars: Shock effects of basin-forming impacts, *Geophys. Res. Lett.*, *30*(6), 1281, doi:10.1029/2002GL016657.
- Jakosky, B. M., R. O. Pepin, R. E. Johnson, and J. L. Fox (1994), Mars atmospheric loss and isotopic fractionation by solar wind-induced sputtering and photochemical escape, *Icarus*, *111*, 271–288.
- Johnson, C. L., and R. J. Phillips (2005), Evolution of the Tharsis region of Mars: Insights from magnetic field observations, *Earth Planet. Sci. Lett.*, *230*, 241–254.
- Kuang, W., W. Jiang, and T. Wang (2008), Sudden termination of Martian dynamo?: Implications from subcritical dynamo simulations, *Geophys. Res. Lett.*, doi:10.1029/2008GL034183, in press.
- Langlais, B., and M. Purucker (2007), A polar magnetic paleopole associated with Apollinaris Patera, Mars, *Planet. Space Sci.*, *55*, 270–279.
- Lillis, R. J., D. L. Mitchell, R. P. Lin, and M. H. Acuña (2008a), Electron reflectometry in the Martian atmosphere, *Icarus*, *194*, 544–561, doi:10.1016/j.icarus.2007.09.030.

- Lillis, R. J., H. V. Frey, M. Manga, D. L. Mitchell, R. P. Lin, M. H. Acuña, and S. W. Bougher (2008b), An improved crustal magnetic field map of Mars from electron reflectometry: Highland volcano magmatic history and the end of the Martian dynamo, *Icarus*, *194*, 575–596, doi:10.1016/j.icarus.2007.09.032.
- McClelland, E. (1996), Theory of CRM acquired by grain growth, and its implications for TRM discrimination and paleointensity determination in igneous rocks, *Geophys. J. Int.*, *126*, 271–280.
- Mohit, P. S., and J. Arkani-Hamed (2004), Impact demagnetization of the Martian crust, *Icarus*, *168*, 305–317.
- Mustard, J. F., F. Poulet, J. W. Head, N. Mangold, J.-P. Bibring, S. M. Pelkey, C. I. Fassett, Y. Langevin, and G. Neukum (2007), Mineralogy of the Nili Fossae region with OMEGA/Mars Express data: 1. Ancient impact melt in the Isidis Basin and implications for the transition from the Noachian to Hesperian, *J. Geophys. Res.*, *112*, E08S03, doi:10.1029/2006JE002834.
- Neumann, G. A., M. T. Zuber, M. A. Wieczorek, P. J. McGovern, F. G. Lemoine, and D. E. Smith (2004), Crustal structure of Mars from gravity and topography, *J. Geophys. Res.*, *109*, E08002, doi:10.1029/2004JE002262.
- Ogawa, Y., and M. Manga (2007), Thermal demagnetization of Martian upper crust by magma intrusion, *Geophys. Res. Lett.*, *34*, L16302, doi:10.1029/2007GL030565.
- Phillips, R. J., et al. (2001), Ancient geodynamics and global-scale hydrology on Mars, *Science*, *291*, 2587–2591, doi:10.1126/science.1058701.
- Saar, M. O., and M. Manga (2004), Depth dependence of permeability in the Oregon Cascades inferred from hydrogeologic, thermal, seismic, and magmatic modeling constraints, *J. Geophys. Res.*, *109*, B04204, doi:10.1029/2003JB002855.
- Scott, E. R. D., and M. Fuller (2004), A possible source for the Martian crustal magnetic field, *Earth Planet. Sci. Lett.*, *220*, 83–90.
- Stevenson, D. J. (2003), Planetary magnetic fields, *Earth Planet. Sci. Lett.*, *208*, 1–11.
- Tanaka, K. L. (1986), The stratigraphy of Mars, *J. Geophys. Res.*, *91*, E139–E158.
-
- H. V. Frey, Planetary Geodynamics Laboratory, NASA Goddard Space Flight Center, Mail Code 698, Greenbelt, MD 20771, USA.
- R. J. Lillis, Space Sciences Laboratory, University of California, 7 Gauss Way, Berkeley, CA 94720, USA. (rlillis@ssl.berkeley.edu)
- M. Manga, Department of Earth and Planetary Science, University of California, 307 McCone Hall, Berkeley, CA 94720, USA.